Acta Astronautica 132 (2017) 13–18

Contents lists available at ScienceDirect

Acta Astronautica

journal homepage: www.elsevier.com/locate/actaastro

Effect of the rail unevenness on the pointing accuracy of large radio telescope

Na Li*, Jiang Wu, Bao-Yan Duan, Cong-Si Wang

School of Mechanical Electronic Engineering, Xidian University, Shannxi 710071, China

ARTICLE INFO

Keywords:
Rail unevenness
Pointing accuracy
Large radio telescope
Coarse-fine mixed
Modeling

ABSTRACT

Considering the stringent requirement of the pointing accuracy up to 2.5″ of the World largest full steerable telescope, this paper presents a coarse-fine mixed model to describe the azimuth rail unevenness. First, the coarse-fine mixed model is proposed. In the model, the trigonometric function is utilized to describe the error with long wavelength whilst the fractal function is used for the short wavelength errors, separately. Then the mathematic model of the pointing accuracy is developed mathematically. Finally, the coarse-fine model and point accuracy model are applied to Green Bank Telescope with valuable result. This paved the way for predicting point error of Qi Tai Telescope.

1. Introduction

Over the last two decades, many countries have been racing to construct the large radio telescopes, such as the Green Bank Telescope (GBT) in America [1], the Effelsberg Telescope in Germany [2] and the Sardinia Radio Telescope in Italy [3]. From 2014, China has been planning to build the Qi Tai telescope (QTT), which will be a fully steerable telescope with the world's largest aperture (110 m). QTT is designed to work from 150 MHz to 115 GHz, which results in a repeatable pointing accuracy requirement of 1.19 s. The whole telescope structure is about 6000 t in weight and as high as a 30-floor building [4]. Therefore, such a strict pointing accuracy requirement imposes considerable difficulties on the design of QTT [5]. For the factors affecting the pointing accuracy, the telescope itself is absolutely the most important one, such as the inertia and elastic deformation of the mount, the reflector and the rail. Currently, high-precision ratio telescopes typically adopt the completely-welded rails. Compared to non-welded rails, it avoids the large deformations at rail junctions, and thereby prolongs the telescopes service life [6]. However, during the manufacturing and welding processes, it is inevitable that errors such as surface roughness and rail stress deformation are produced [7]. These errors are collectively referred to as rail unevenness. It can directly lead to the azimuth frame errors in azimuth and pitching axis, and then affect the pointing accuracy of telescope [8].

As early as 2000, Gawronski began to notice the effect of rail unevenness on radio telescope. By the aid of an inclinometer, he converted the measured unevenness data into errors of the telescope's azimuth and pitch angles in accordance with their geometric relationship [9]. Additionally, Pisanu considered the combined effects of the deformation of the azimuth frame on pointing accuracy, which was induced by rail unevenness and temperature drift [10]. Kong performed the testing experiment on the rail unevenness and pointing accuracy and analyzed the correlation between them [11]. Besides, some researchers indirectly introduced the non-linear rail errors into the construction of a telescope's pointing model [12]. Although many fruitful results have been achieved [13], the description of rail unevenness is too ambiguous, leading to immense fitting errors and thereby severely affecting a telescope's ultimate pointing accuracy. An accurate model of rail unevenness, which is required in studies involving the effects of rail unevenness on pointing accuracy, has not yet been constructed. And so a model for antenna pointing errors, in which rail unevenness is taken into account, has still not to been established. The qualitative relationship between rail unevenness and the pointing accuracy of the antenna have not been found fundamentally.

Aimed at solving the aforementioned problems, this article describes the rail unevenness using the Fourier series and the fractal function, and innovatively proposed the coarse-fine mixed description model. Finally, an influence relationship model of the rail unevenness on the pointing accuracy was established based on the mixed model.

2. Coarse-fine mixed modeling of the rail unevenness

Errors that lead to rail unevenness primarily originate from two aspects – the surface roughness produced in the machining process of a single rail and the deformations produced during the welding process

* Corresponding author.
E-mail addresses: lina@mail.xidian.edu.cn (N. Li), 836640638@qq.com (J. Wu), byduan@xidian.edu.cn (B.-Y. Duan), congsiwang@163.com (C.-S. Wang).

http://dx.doi.org/10.1016/j.actaastro.2016.12.005
Received 12 July 2016; Accepted 1 December 2016
Available online 05 December 2016

and post-processing. These two different kinds of surface error have different characteristics [14,15]. The surface roughness is randomness, high-frequency, low-amplitude, and small scale, while the deformation is systematic, low frequency, and large amplitude. Based on these distribution features, the large-scale deformation of rail unevenness was fitted using the Fourier series [16]. Next, the Weierstrass-Mandelbrot (W-M) fractal function was used to describe the fitting residual error, and then, fitting function of the small-scale roughness was conducted [17]. Finally, the coarse-fine mixed model of rail unevenness was established, as shown below in Eq. (1).

$$\begin{aligned} F(x) &= f_1(x) + \textstyle\sum_{i=1}^{k} f_2^i(A_i, D_i, L_i, x_0^i, y_0^i) \\ &= (a_0 + \textstyle\sum_{n=1}^{m} [a_n \cos(n\omega_0 x) + b_n \sin(n\omega_0 x)]) \\ &\quad + (\textstyle\sum_{i=1}^{k} f_2^i(A_i, D_i, L_i, x_0^i, y_0^i)) \\ f_2^i(A_i, D_i, L_i, x_0^i, y_0^i) &= A_i^{(D_i-1)} \textstyle\sum_{j=n_{1i}}^{M_i} \frac{1}{\gamma^{(2-D_i)j}} \cos(2\pi\gamma^j (x + x_0^i)) + y_0^i \\ n_{1i} &= \lg(1/L_i)/lg(\gamma) \\ M_i &= \lg(N\gamma^{n_{1i}}/2)/lg(\gamma) \end{aligned} \tag{1}$$

where, $f_1(x)$ denotes the Fourier series; $a_0, a_1, \ldots, a_n, b_1, \ldots, b_n$ denotes the undetermined coefficient of $f_1(x)$; m denotes the expansion order of $f_1(x)$; ω_0 denotes the fundamental frequency of $f_1(x)$; S denotes the rail length described by $F(x)$ and is generally set as one third of the rail's overall length; k denotes the number of rail segments when the W-M fractal function is used for fitting rail unevenness; l denotes the fitting length of f_2^i ($k = S/l$) and is set as a round number; $f_2^i(A_i, D_i, L_i, x_0^i, y_0^i)$ denotes the i-th segment of the W-M fractal function $f_2(x)$; A_i denotes the amplitude height coefficient of $f_2(x)$, reflects the value of f_2^i, and determines the specific size of f_2^i; L_i denotes the sampling length of $f_2(x)$; D_i denotes the fractal dimension of $f_2(x)$; y_0^i and x_0^i denote the longitudinal and lateral displacements of $f_2(x)$, respectively.

As shown in Eq. (1), the Fourier series $f_1(x)$ and the W-M fractal function $f_2(x)$ codetermine the fitting precision of rail unevenness. Moreover, higher expansion order of the Fourier series (m), will result in higher the fitting precision is. Similarly, shorter the sampling length of the fractal function (L), will result in the higher the fitting precision is. In this work, the sampling length of the Weierstrass-Mandelbrot (W-M) fractal function (L) equals the fitting length of the small-scale function, and so determining the values of m and L is the key to determining the unevenness model [18]. The determination methods for these two key parameters are described in detail below [19]. The optimization model based on the W-M fractal function can be described as:

$$F(y) = \sqrt{[\sum_{j=1}^{N} (f_2^i(x_j, y) - y(x_j))^2]/N} \tag{2}$$

$$f_2(x) = A^{(D-1)} \sum_{n=n1}^{M} \frac{1}{\gamma^{(2-D)n}} \cos(2\pi\gamma^n (x + \Delta x)) + \Delta y \tag{3}$$

$$\begin{aligned} &\textit{Find} && y = (A_i, D_i, L_i, x_0^i, y_0^i)^T \\ &\textit{Min.} && F(y) = \sqrt{[\textstyle\sum_{j=1}^{N} (f_2^i(x_j, y) - y(x_j))^2]/N} \\ &\textit{S. T.} && 0 < x_0^i < x_{\max} \\ &&& L_{\min} < L_i < L_{\max} \\ &&& y_{\min} < y_0^i < y_{\max} \\ &&& A_{\min} < A_2^i < A_{\max} \\ &&& D_{\min} < D_i < D_{\max} \end{aligned} \tag{4}$$

The upper and lower limits of the variables were determined based on their physical meanings. The physical meanings and the determination methods for the related parameters in the optimization model of fractal function are described in the Fig. 1.

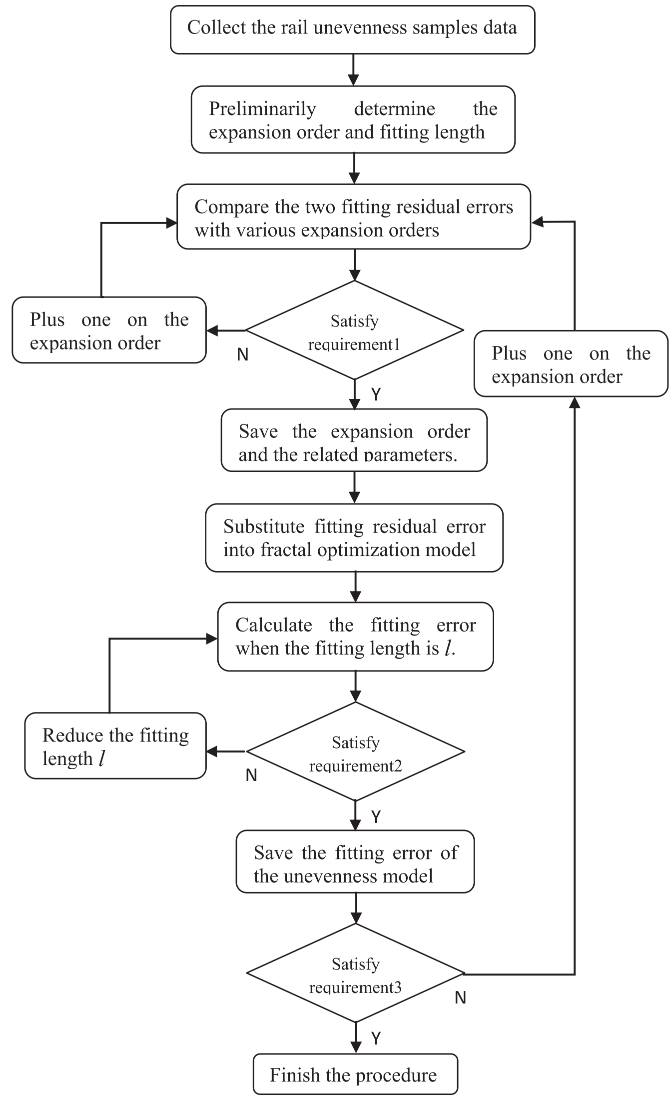

Fig. 1. Displays the detailed process for determining the parameters.

3. Effects of rail unevenness on the QTT's pointing accuracy

3.1. Effect of the rail unevenness on the azimuth frame error

To describe telescope's various errors and investigate their effects on the pointing accuracy, four coordinate systems were constructed, as shown in Fig. 2, the detailed descriptions of these coordinate systems are provided below:

$OXYZ$- Geodetic coordinate system, in which the origin is located at the center of the azimuth orbit, the Z-axis is perpendicular to the ground, and the negative direction of the Y-axis points to true north.

$O_aX_aY_aZ_a$- Coordinate system rigidly connected to the azimuth axis, in which the origin is located at the center of the azimuth orbit and the Z_a-axis coincides with the azimuth axis. Overall, the coordinate follows the rotation and deflection of the azimuth axis. When the telescope has no errors along the azimuth axis and the azimuth angle equals zero (i.e., $A = 0^{\circ}$), $O_aX_aY_aZ_a$is identical to $OXYZ$.

$O_eX_eY_eZ_e$-Coordinate system rigidly connected with the pitch axis in which the origin is located at the middle of the pitch axis and the X_e-axis coincides with the pitch axis. Overall, the coordinate follows the rotation and deflection of the pitch axis. When the telescope has no axis errors and the pitch angle and azimuth angle equal 90° and 0°, respectively, $O_eX_eY_eZ_e$ only differs from $OXYZ$ along the direction of the Z-axis with a difference of the height of the azimuth axis h.